Structure and magnetic properties of iron nitride thin films on Cu(001)

Yasumasa Takagi,[1,2] Kyohei Isami,[2] Isamu Yamamoto,[1] Takeshi Nakagawa,[1,2] and Toshihiko Yokoyama[1,2,*]
[1]*Department of Materials Molecular Science, Institute for Molecular Science, Myodaiji-cho, Okazaki 444-8585, Japan*
[2]*Department of Structural Molecular Science, The Graduate University for Advanced Studies (SOKENDAI), Myodaiji-cho, Okazaki 444-8585, Japan*

(Received 3 September 2009; revised manuscript received 10 November 2009; published 22 January 2010)

The structural and magnetic properties of iron nitride thin films on a Cu(001) surface were investigated by low-energy electron diffraction (LEED), scanning tunneling microscopy (STM), x-ray absorption spectroscopy, and x-ray magnetic circular dichroism (XMCD). In the STM and LEED observations of 1 and 2 monolayer (ML) films, the nitride films exhibit $p4gm(2\times2)$ reconstructed smooth surfaces without significant amounts of dislocations or islands. The stoichiometry of the 1 ML film was found to be Fe_2N, while that of 2 ML was Fe_4N, consisting of a topmost layer with the Fe_2N composition and a second layer containing Fe atoms only. The XMCD measurements were performed for nitride films up to 4 ML. The angle-dependent XMCD spectra indicate that the films are ferromagnetic, with easy axes along the surface parallel direction. In addition, according to the results of the sum-rule analysis, strong magnetic anisotropy appears in the 1 ML film, where the orbital magnetic moment perpendicular to the surface is almost zero. The total magnetic moment, which is a combination of the spin and orbital magnetic moments, increases with the increase in film thickness up to 3 ML. The magnetic moment for more than 2 ML is ~2.1 μ_B, which is nearly equal to that of bulk γ'-Fe_4N of 2.2 μ_B.

DOI: 10.1103/PhysRevB.81.035422 PACS number(s): 75.70.Ak, 68.35.B−, 75.50.Bb, 78.70.Dm

I. INTRODUCTION

Enhancement and suppression of magnetic moments in ultrathin films and a change in magnetic anisotropy by adsorption of atoms are attractive issues for surface magnetism.[1–10] These magnetic properties depend on the kinds of atomic species that are adjacent to a magnetic atom and the interatomic distance.[11–13] It is thus essential to perform combined studies with structural and magnetic properties. In the present study, we focus our attention on iron modified by nitrogen. Bulk iron nitrides are interesting materials because of their excellent magnetic properties such as large saturation magnetization and chemical stability, which are advantages for applications in magnetic storage devices. The iron nitride system shows various kinds of phases in a phase diagram, and the magnetic moments are considerably different from each other.[14,15] Regarding the cubic FeN phases, the γ''-ZnS-type nitride is a nonmagnetic metal, while the γ'''-NaCl-type nitride is an antiferromagnet. According to the Mössbauer results for ζ-Fe_2N, the phase is presumably a very weak itinerant ferromagnet.[16] On the other hand, most of the nitrides on the nitrogen-poor side of the phase diagram are ferromagnetic. For the α''-$Fe_{16}N_2$ phase, the magnetic moment is expected to be 2.4–3.5 μ_B.[17–19] The uncertainty of the reported magnetic moments is caused by the difficulty of obtaining a pure bulk phase of α''-$Fe_{16}N_2$. Besides, the magnetic moment of the γ'-Fe_4N phase is ~2.2 μ_B, which is almost equal to that of elemental α-Fe.[20]

While it is technically difficult to prepare uniform single crystals of iron nitrides, high-quality epitaxial layers of γ'-Fe_4N have successfully been grown on a Cu(001) surface by depositing elemental iron in the presence of a flux of atomic nitrogen from a radio-frequency plasma source.[21,22] In the cubic crystalline structure of γ'-Fe_4N shown in Fig. 1, the Fe atoms form an fcc sublattice, while the N atom is placed at the center of the cubic cell, occupying one of the four octahedral vacant sites. The lattice parameter of γ'-Fe_4N is 3.795 Å, which shows a small mismatch with the lattice constant of Cu(001) (3.615 Å). According to the LEED (low-energy electron diffraction) observation combined with Auger electron spectroscopy, the surface of the film formed on the Cu(001) substrate displays a $c(2\times2)$ or $p4gm(2\times2)$ symmetry, depending on the amount of N atoms near the surface.[22] The $c(2\times2)$ phase seems to be formed with less N, while the $p4gm(2\times2)$ phase seem to requires more N. A more detailed morphology and its electronic structure were investigated by scanning tunnel microscopy (STM), low-energy ion scattering, and x-ray and ultraviolet photoelectron spectroscopy.[23–25] In addition, magnetic anisotropy of the films was studied *ex situ* by vectorial Kerr magnetometry.[26,27] However, the quantitative magnetic properties of the ultrathin iron nitride films have not been investigated so far.

In the present study, we investigate the morphology of iron nitride thin films formed on Cu(001) by LEED, STM, and x-ray absorption spectroscopy (XAS), while the magnetic properties have been studied by *in situ* x-ray magnetic

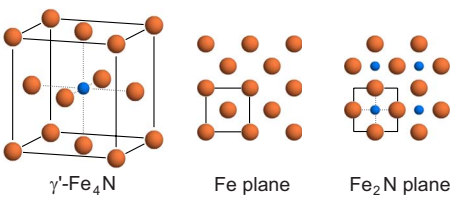

FIG. 1. (Color online) Crystalline structure of γ'-Fe_4N. Large orange and small blue spheres represent Fe and N atoms, respectively. The center and right panels show the two different planes along the [001] direction.

circular dichroism (XMCD) measurements. The STM observation shows that the 1–2 monolayer (ML) iron nitride films provide smooth surfaces without significant dislocations or islands. The structures of films are determined quantitatively by the tensor LEED analysis for *I-V* curves. The results elucidate that the surface of the 1 ML film is reconstructed to $p4gm(2\times2)$ and that its composition ratio of Fe and N is 2:1. In the case of a 2 ML film, the topmost layer shows a $p4gm(2\times2)$ structure with the Fe_2N composition similar to the 1 ML film, while the second layer consists of a pure Fe layer epitaxially grown on Cu(001). Thus, the composition ratio of the 2 ML film is Fe:N=4:1 altogether and its structure corresponds to one period of γ'-Fe_4N crystalline structure along the (001) direction. The XMCD measurements indicate that these iron nitride films are ferromagnetic with easy axes along the surface parallel direction. The spin and orbital magnetic moments are evaluated directly using the spin and orbital sum-rules.[28,29] Large magnetic anisotropy is observed in the 1 ML film, where the orbital magnetic moment perpendicular to the surface is almost zero due to strong chemical bonding between Fe and N atoms located almost within the same surface plane. The magnetic moment increases with the film thickness, and for 3 and 4 ML it is almost equal to that of bulk γ'-Fe_4N.

II. EXPERIMENTS

The STM, LEED, XAS, and XMCD measurements were performed in two independent ultrahigh vacuum (UHV) chambers with the same sample preparation condition. A Cu(001) single crystal was cleaned by Ar^+ ion sputtering and 900 K annealing cycles in the UHV chamber with a base pressure of $\sim1\times10^{-10}$ Torr. The iron nitride films were prepared in the following steps. The clean Cu(001) surface was exposed to low-energy ($\sim$150 eV) N^+ bombardment with a pressure of 5×10^{-8} Torr at room temperature (RT) for 15 min. 1 ML Fe (99.99%) was subsequently deposited on the N-adsorbed Cu(001) substrate at RT from an electron-beam evaporator. Finally, the 1 ML iron nitride film was formed after annealing the sample in UHV at 720 K for 10 min. This process was repeated for more than 1 ML. Note that one monolayer is defined as an atomic concentration of Fe of 1.53×10^{15} atom/cm^2, which corresponds to the atomic density of the Cu(001) surface, and that the Fe thickness was calibrated using the reflection high-energy electron diffraction oscillation observed in Fe deposition on clean Cu(001).[5]

The structure of the film surface was observed by STM with an electrochemically etched tungsten tip. All STM image were taken in a constant-current mode at RT. LEED patterns for the *I-V* measurements were recorded by a computer-controlled CCD camera at the sample temperature of 100 K. A Barbieri/Van Hove symmetrized automated tensor LEED package[30] was used to simulate *I-V* curves for structure models. The surface structure model was optimized by minimizing the Pendry *R* factor (R_p).[31]

The *in situ* Fe *L*-edge XAS and XMCD measurements were performed at the bending magnet station BL 4B at UVSOR-II.[32] The XMCD measurement system with a split superconducting magnet (maximum magnetic field of ±7 T)

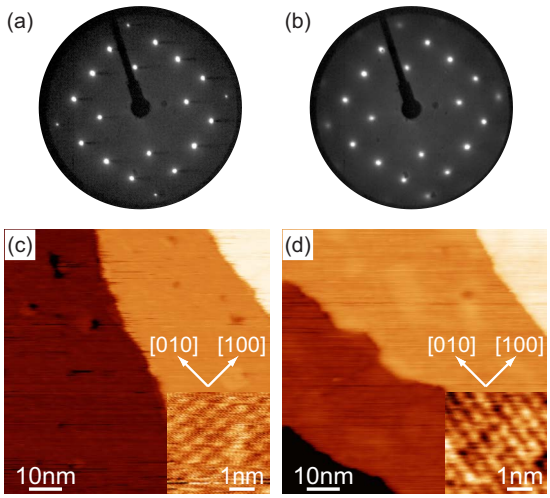

FIG. 2. (Color online) (a,b) LEED patterns of the 1 ML (a) and 2 ML (b) iron nitride films formed on Cu(001) with the incident electron energy of 100 eV. (c,d) STM images of 1 ML (c) and 2 ML (d) iron nitride films on Cu(001). The image size is 80×80 nm^2. The inset shows magnified image (4×4 nm^2) of the surface on the terrace.

was reported in Ref. 33 in detail. The XAS and XMCD spectra were recorded with a total electron yield mode by detecting a drain current from the sample at a temperature of 5 K. The circular polarization factor was estimated to be $P_c=0.57$, and the XMCD spectra were taken by switching the magnetic field *H*, leaving the x-ray helicity unchanged. The angular dependence of the XMCD spectra was examined at the x-ray incidence polar angles $\theta=0°$ (normal x-ray incidence) and $\theta=55°$ (grazing x-ray incidence). The x-ray propagation vector **k** was set within the $(1\bar{1}0)$ plane of a substrate Cu crystal. The procedure of the XMCD sum-rule analysis is described in Sec. III B.

III. RESULTS AND DISCUSSION

A. Morphology

In this section, we reveal the surface structures of 1 and 2 ML iron nitride films formed on Cu(001) by LEED, STM, and XAS. The LEED patterns of 1 ML and 2 ML iron nitride films are shown in Figs. 2(a) and 2(b), respectively. Sharp $p4gm(2\times2)$ patterns were observed in a wide energy range from 40 to 400 eV, indicating the growth of smooth and homogeneous films on Cu(001). No other pattern has been observed in a 1 or 2 ML iron nitride film, although the $c(2\times2)$ LEED pattern was reported in film with a thickness up to 300 Å when the relative amount of N at the surface was small.[22] This fact indicates that the Fe/N composition ratio is constant in the early stages such as 1 ML and 2 ML, because in thinner films there is the less freedom of atomic displacements than in thicker films. This can be confirmed by the STM images in Figs. 2(c) and 2(d), where wide terraces with a monoatomic step are clearly seen. The images show uniform and smooth surfaces without significant dislocations and islands. The insets at the right bottom in Figs. 2(c) and 2(d) are the enlarged images in the terrace. The images ex-

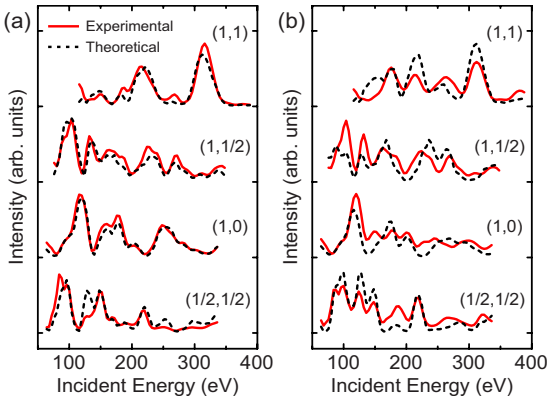

FIG. 3. (Color online) Comparison between the experimental (solid red line) and simulated (dashed black line) LEED *I-V* curves for $p4gm(2\times2)$ structures of 1 ML (a) and 2 ML (b) iron nitride films on Cu(001).

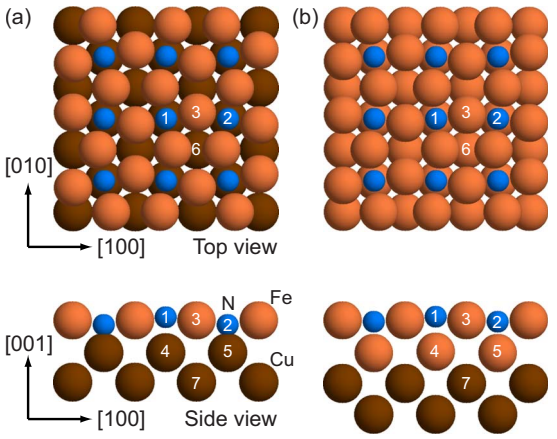

FIG. 4. (Color online) Top and side views of the determined $p4gm(2\times2)$ structures of 1 ML (a) and 2 ML (b) iron nitride films formed on Cu(001).

hibit a periodic corrugation corresponding to a $c(2\times2)$ superstructure with respect to the Cu(001) substrate in contrast to the observed $p4gm(2\times2)$ LEED pattern. The apparent corrugation may not accurately depict the structure due to the low resolution of the images. A wavy pattern of the atomic arrangement of the $p4gm(2\times2)$ reconstruction[24] could be seen by STM observation at higher resolution.

The composition ratios of the FeN films are approximated from the XAS edge-jump measurements because the Fe *L* (~707 eV) and N *K* (~396 eV) edge jumps normalized with the Cu *L* (~930 eV) one are proportional to the number of these atoms in the films when the film is a few monolayers thick. We measured the XAS at the normal incidences of linear x-rays for 1 and 2 ML iron nitride films. The N *K*-edge jump normalized with Cu is 0.021 for 1 ML, which is almost the same as that in the reference material Cu(001)-$c(2\times2)$N (0.022), where the 0.5 ML N atoms are located at the fourfold hollow site.[34] For the 2 ML film, the N *K*-edge jump is again 0.021, while the Fe *L*-edge jump increases twice from 0.10 for 1 ML to 0.19 for 2 ML. Assuming that Fe forms an fcc structure grown epitaxially on Cu(001), the present results of the XAS edge-jump measurements indicate that the compositions of 1 and 2 ML iron nitride films are Fe:N=2:1 and 4:1, respectively.

The LEED *I-V* analysis was performed to determine quantitatively the structures of thin films. The *I-V* curves of four diffraction spots, (1/2,1/2), (1,0), (1,1/2), (1,1) in the $p4gm(2\times2)$ pattern were recorded with normal electron incidence. The total energy range of the *I-V* curves used in the analysis is 1120 eV. The atom positions of Cu(001)-$c(2\times2)$N were adopted as a reference structure, and the atoms from the first to third layers were displaced for the structure optimization.

By considering the $p4gm(2\times2)$ superstructure and the Fe/N composition ratio, we modeled a 1 ML iron nitride film consisting of a Fe_2N layer on Cu(001), where the N atoms are located at the fourfold hollow site of 1 ML fcc Fe and the four Fe atoms rotate around the N atom within the surface plane. In Fig. 3(a), the calculated *I-V* curves are compared with the experimental ones for 1 ML. The resultant R_p value is 0.16, which is satisfactorily small. For the 2 ML iron nitride film, by taking into account the Fe/N composition ratio (Fe:N=4:1), we adopted a model consisting of the Fe_2N layer similar to the 1 ML film as the topmost layer and a pure Fe layer as the second layer, because N is likely to segregate to the topmost layer to decrease the surface energy. The calculated curves for 2 ML are shown in Fig. 3(b) with the experimental ones. The resulting R_p value is 0.31, which is larger than the value for 1 ML. However, using the other model where the topmost layer is pure Fe and N atoms exist only in the second layer, the resulting R_p value is at least 0.49. Thus, we conclude that the former model is more probable. The reason for the less-optimal value in 2 ML than in 1 ML may be that the actual film with an average thickness of 2 ML contains various thicknesses, such as a mixture of 1 to 3 monolayers, especially around the step edges. The signals from these contributions may have been superimposed, resulting in a worse R_p value.

The results of LEED *I-V* analysis lead to the conclusion that the 1 ML film has a $p4gm(2\times2)$ structure with a composition ratio of Fe:N=2:1. On the other hand, the composition ratio of the 2 ML film is Fe:N=4:1, where the topmost layer has a $p4gm(2\times2)$ structure similar to the that of the 1 ML film and the second layer is a pure Fe layer. The models of the best fit $p4gm(2\times2)$ structures are shown in Fig. 4, and the optimized parameters with atom positions of the reference structure are listed in Table I. These structures can be thought to have distorted γ'-Fe_4N phases. The 1 ML film has the same composition as the Fe_2N layer of γ'-Fe_4N, and the structure of the 2 ML film corresponds to a period of γ'-Fe_4N along the (001) direction, which contains Fe_2N and pure Fe layers.

The Fe atoms at the topmost layer (No. 3) of the 1 ML film move from the midpoint between the two N atoms (Nos. 1 and 2) by 0.39 Å along the $\pm y$ direction. It is interesting to note that the N atoms move upward (No. 1) and the N atoms move upward and downward alternately from the top Fe layer by ~0.2 Å to relax the lattice mismatch of ~5% between bulk γ'-Fe_4N and Cu(001), although both the N atoms have the same circumstances. On the other hand, the atoms below the second layer almost keep the reference positions. Namely, the interface strain can be relaxed only in

TABLE I. Optimized structural parameters of the $p4gm(2\times2)$ iron nitride films formed on Cu(001). The number in the first column (No.) corresponds to the atom indicated in Fig. 4. The atom labeled 1 is located at the origin of the coordinates. The x, y, and z coordinates imply the [100], [010], and [001] directions, respectively. The displacements are given with respect to the reference structure, which is the same atom positions as Cu(001)-$c(2\times2)$N. No displacement along the x direction takes place because of the $p4gm(2\times2)$ symmetry.

	Reference Structure (Å)			Displacement (Å)			
				1 ML		2 ML	
No.	x	y	z	Δy	Δz	Δy	Δz
1	0	0	0	0	0.23(8)	0	0.27(7)
2	3.62	0	0	0	−0.24(3)	0	−0.04(3)
3	1.81	0	0	0.39(5)	0.04(9)	0.26(8)	0.05(8)
4	0	0	−1.81	0	−0.04(3)	0	0.05(3)
5	3.62	0	−1.81	0	−0.02(3)	0	−0.04(2)
6	1.81	−1.81	−1.81	0	−0.05(2)	0	−0.03(3)
7	1.81	0	−3.62	0.03(7)	0.05(2)	0.08(9)	−0.03(3)

the topmost layer to reconstruct the surface into the $p4gm(2\times2)$ structure. The surface relaxation allows the formation of flat iron nitride films on Cu(001) without defects or dislocations, as seen in Fig. 2.

At the end of this section, we mention briefly the inactivation and stability of the surface. No contamination appears in the STM images during the measurement for a day, and a sharp LEED pattern was maintained after the STM measurements. Regarding the thermostability of the surface, the $p4gm(2\times2)$ structure appears after the annealing at 780 K, which is higher than the N desorption temperature from the Cu(001)-$c(2\times2)$N surface.[35] This implies that the N–Fe bond is stronger than the N–Cu bond. In addition, after the iron nitride films form on the surface, no Fe atom is intermixed with the Cu substrate during annealing.

B. Magnetic properties

This section discusses the magnetic properties of iron nitride films in thicknesses ranging from 1 to 4 ML by XAS and XMCD measurements. The structures of the 1 and 2 ML films were determined in the previous section. The LEED patterns of the 3 and 4 ML films also showed the $p4gm(2\times2)$ symmetry. The composition Fe/N ratios are Fe:N =4:1, similar to the case with 2 ML, verified from the results of the XAS edge-jump measurements. Since the thick iron nitride films on Cu(001) show the γ'-Fe_4N structure,[22] it is reasonable to infer that the structure of the film thicker than 2 ML also has the γ'-Fe_4N structure.

First, we show the circularly polarized Fe $L_{III,II}$-edge XAS of pure iron and iron nitride films on Cu(001) under magnetic field $H=\pm5$ T, taken at normal x-ray incidence (the x-ray helicity and the magnetization perpendicular to the surface) at a temperature of 5 K (Fig. 5). The spectra are normalized with the edge jumps. The spectral features of iron nitride films are clearly different from those of a pure Fe film. A shoulder structure appears at a higher energy side of the main peak at the L_{III} edge. The shoulder structure can be ascribed to the multiplet splitting due to the cationicity of the Fe atoms. Besides, it is clear that the difference between the left- and right-circularly polarized spectra, which corresponds to XMCD, increases with the film thickness.

Figure 6 gives typical magnetization curves obtained by recording the electron yield with the photon energy fixed at the Fe L_{III} peak top (~707 eV). The amplitude corresponds

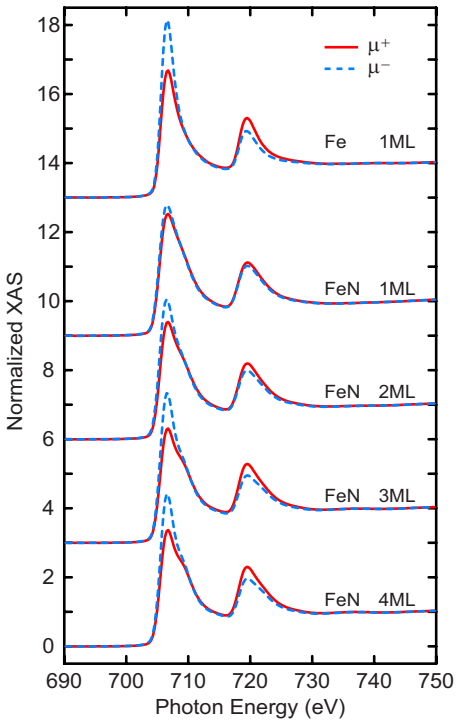

FIG. 5. (Color online) Circularly polarized XAS at the Fe $L_{III,II}$-edges of pure iron and 1–4 ML iron nitride films on Cu(001), taken at normal x-ray incidence. μ^+ (μ^-) is the spectrum with the electron spin direction parallel (antiparallel) to the x-ray helicity.

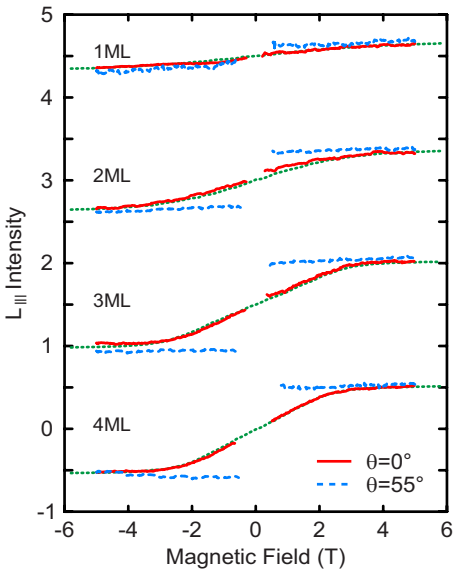

FIG. 6. (Color online) Magnetization curves of 1–4 ML iron nitride films obtained by recording the electron yield with the photon energy fixed at the Fe L_{III} peak top (~707 eV) for the x-ray incident angles $\theta=0°$ (normal x-ray incidence, red solid line) and $\theta=55°$ (grazing x-ray incidence, blue dashed line). The simulated magnetization curves using a simple magnetic anisotropy model are also depicted (green dotted lines).

to the difference in the L_{III} peak intensity of XAS normalized with the edge jump of the spectrum at $H=0$, indicating a larger magnetic moment at a larger thickness. The magnetization curve provides information on magnetic anisotropy and is also useful for estimating the saturated magnetization required in the XMCD analysis. The data in the vicinity of $H=0$ are omitted due to strong suppression of the electron yield by the Lorentz force. All the grazing incidence ($\theta=55°$) curves show steplike features with a constant intensity at $|H|>0.5$ T, while the smoothed shapes of the magnetization curves appear in the normal incidence ($\theta=0°$) curves. It is concluded that these films are ferromagnetic with the magnetic easy axes parallel to the surface. In contrast to a report that the magnetization of bulk Fe_2N is very weak,[16] the 1 ML iron nitride film with a stoichiometry of Fe_2N is found to be ferromagnetic. The structure of the 1 ML iron nitride film on Cu(001) is the tetragonal structure shown in Fig. 4(a), while bulk Fe_2N is the α-PbO_2 type orthorhombic structure.[36] The structural difference between the film and the bulk may cause the difference in the magnetic properties.

The magnetization curves measured at the normal x-ray incidence ($\theta=0°$) were simulated using a simple second order magnetic anisotropy model. The magnetic anisotropy energy E_a is phenomenologically given as

$$E_a = \left(K_u + \frac{M_s^2}{2\mu_0}\right)\cos^2\theta - M_s H\cos(\theta_M - \theta), \qquad (1)$$

where θ_M is the polar angle of the magnetization M_s, K_u is the uniaxial anisotropy constant, and μ_0 is the vacuum permeability. Since the round curvature indicates the finite-temperature effect due to the small size of the magnetic domain, the classical Boltzmann distribution function $\rho=\exp(-NE_a/k_BT)$ was assumed in the simulation, where k_B is the Boltzmann constant and N is the number of atoms in one magnetic domain. The simulations were performed using the Monte Carlo method. Here the magnetization M_s is estimated from the result of the XMCD analysis discussed later. The results of the simulated magnetization curve are also shown in Fig. 6, and the estimated parameters are listed in Table II.

TABLE II. Uniaxial anisotropy constants K_u, domain sizes N estimated from the simulations of the magnetization curves in Fig. 6. The magnetization M_s is determined from the XMCD analysis and is also listed here.

	K_u (meV/atom)	N (atom)	M_s (μ_B/atom)
1 ML	0.114(20)	10(5)	0.73(10)
2 ML	0.102(20)	10(5)	1.47(10)
3 ML	0.092(20)	25(5)	2.17(10)
4 ML	0.048(20)	25(5)	2.12(10)

The XMCD spectra of the Fe L-edge at $H=\pm5$ T are shown in Fig. 7. The intensity of the XMCD signals increases with the film thickness. According to the above results of the magnetization curves at an x-ray incident angle $\theta=0°$, the magnetizations of all of the films are almost saturated under $H=5$ T. A sum-rule analysis was performed using the formulas of the orbital magnetic moment (m_{orb}) and the spin magnetic moment (m_{spin}).

For the evaluation of the magnetic moments, the d-hole number n_d is required, which is experimentally estimated by using the formula as

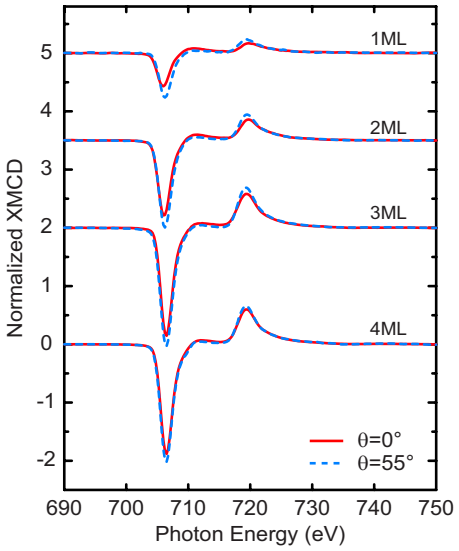

FIG. 7. (Color online) Fe L-edge XMCD spectra of 1–4 ML iron nitride films at $H=\pm5$ T for the x-ray incident angles $\theta=0°$ (normal x-ray incidence, red solid line) and $\theta=55°$ (grazing x-ray incidence, blue dashed line), normalized with the $L_{\mathrm{III,II}}$-edge jumps.

TABLE III. Results of the sum-rule analysis of iron nitride films. Average spin (m_{spin}) and orbital (m_{orb}) magnetic moments of Fe are given, which are obtained from the experimental XMCD spectra in Fig. 7.

	n_d	$m_{spin}(\mu_B)$	$m_{orb}^{\parallel}(\mu_B)$	$m_{orb}^{\perp}(\mu_B)$	$m_T^{\parallel}(\mu_B)$	$m_T^{\perp}(\mu_B)$
1 ML	3.87(15)	0.73(10)	0.07(5)	0.00(5)	−0.000(5)	0.000(5)
2 ML	3.80(15)	1.38(10)	0.18(5)	0.11(5)	0.006(5)	−0.011(5)
3 ML	3.80(15)	2.05(10)	0.25(5)	0.15(5)	0.008(5)	−0.016(5)
4 ML	3.88(15)	1.98(10)	0.24(5)	0.17(5)	0.008(5)	−0.016(5)

$$n_d = C\int_{L_{III}+L_{II}} (\mu^{av} - \mu^{BG})dE, \tag{2}$$

where $\mu^{av}=(\mu^+ + \mu^-)/2$ and μ^{BG} is the background absorption spectrum expressed by the two step functions. The proportional constant C in Eq. (2) is obtained by the standard spectrum of some reference metal whose n_d is known. In the present analysis, the XMCD spectrum of bulk *bcc* Fe (n_d is assumed to be 3.40) was used as the standard.

The effective spin magnetic moment $m_{spin}^{eff}=m_{spin}+7m_T$ (m_T is the magnetic dipole term) and m_{orb} are evaluated as

$$\frac{m_{spin}^{eff}}{\mu_B} = -\frac{C}{3}\left(\int_{L_{III}} \Delta\mu dE - 2\int_{L_{II}} \Delta\mu dE\right) \tag{3}$$

and

$$\frac{m_{orb}}{\mu_B} = -\frac{2C}{3}\int_{L_{III}+L_{II}} \Delta\mu dE, \tag{4}$$

where $\Delta\mu$ is the XMCD (the difference between μ^+ and μ^-), and μ_B is the Bohr magneton. m_T can be estimated by measuring the angle dependence of the XMCD spectra. Stöhr and Köning[37] proposed the important formulas as

$$m_{orb}(\theta_m) = m_{orb}^{\perp}\cos^2\theta_m + m_{orb}^{\parallel}\sin^2\theta_m, \tag{5}$$

$$m_T(\theta_m) = m_T^{\perp}\cos^2\theta_m + m_T^{\parallel}\sin^2\theta_m, \tag{6}$$

and

$$0 = m_T^{\perp} + 2m_T^{\parallel}, \tag{7}$$

where θ_m denotes the polar angle of the magnetic moment m, and the superscripts $\perp$ and $\parallel$ denote the directions of the magnetic moments perpendicular and parallel to the surface, respectively. We can evaluate all the magnetic moment by using the numerical values obtained by the sum-rule analysis for the XMCD data of two x-ray incident angles $\theta=0°$ and 55°. The evaluated magnetic moments are listed in Table III.

The considerably smaller magnetic moments in the 1 ML iron nitride films than in a pure iron film (the moment of bulk α-Fe is 2.2 μ_B) is ascribed to the strong chemical bonding between Fe and N, which is also indicated by the shoulder peak in XAS spectra in Fig. 5. The perpendicular orbital magnetic moment in 1 ML is almost zero, indicating strong in-plane magnetic anisotropy. As seen in Fig. 4(a), the N atoms in the 1 ML film are located almost in the same plane of the topmost Fe layer. In this arrangement, the perpendicular angular momentum of the Fe atom (electron rotation within the surface plane) is effectively quenched by the N atom, leading to an almost zero perpendicular orbital magnetic moment and a strong in-plane magnetic anisotropy.

When the thickness of the film varies from 1 to 2 ML, the Fe/N stoichiometry changes from 2:1 to 4:1. According to the film structures seen in Fig. 4, all the Fe atoms in the first layer of the 2 ML film have chemical bonds with two nearest-neighbor N atoms, which are almost within the same surface plane as in the 1 ML film, while the half of Fe atoms in the second layer have a chemical bond with only one nearest-neighbor N atom in the vertical direction; the other half do not directly interact with the N atoms. Thereby, the average m_{spin} value increases from 0.73 μ_B for 1 ML to 1.38 μ_B for 2 ML, although the magnetic moment is still smaller than the bulk γ'-Fe_4N of 2.2 μ_B. When the thickness is more than 2 ML, the increase in the average magnetic moment is rather saturated, approaching the bulk one of γ'-Fe_4N.

In many thin films, enhancement of the magnetic moments has been reported and could be ascribed to the reduced atomic coordination of the surface atoms.[2,33] The results of the first-principle calculations for a γ'-Fe_4N surface possessing the Fe_2N stoichiometry indicate that the magnetic moment of the surface Fe atom is larger than that in the bulk while that of the second layer Fe atom is smaller.[13] Altogether, the average magnetic moment around the surface region is almost equal to the bulk value. On the other hand, the magnetic moment of 2 ML obtained in this work is quite small compared to the bulk value. This discrepancy might be attributed to a shorter N-Fe distance in the thin film than that in the bulk Fe_4N, because the lattice parameter of the Cu(001) surface is smaller than that in the bulk γ'-Fe_4N. A shorter N-Fe distance may result in the reduction in the Fe magnetic moment. Moreover, the present study has elucidated the structural difference between the iron nitride film and the bulk γ'-Fe_4N. The Fe magnetic moment in the $p4gm(2\times2)$ reconstructed structure at the surface could be smaller than that in the ideal $c(2\times2)$ structure that appears ideally at the Fe_2N layer in bulk Fe_4N. On the other hand, the magnetic moments of 3 and 4 ML iron nitrides are nearly equal to the bulk value. This can be attributed to the smaller contribution of the topmost $p4gm(2\times2)$ layer than the inner layers, which have a structure similar to that of bulk γ'-Fe_4N.

Finally, we briefly discuss the uniaxial anisotropy constant (K_u). Bruno[38] theoretically derived the relation between the microscopic orbital magnetic moment and the macroscopic magnetic anisotropy constant as

$$K_u = \frac{\xi}{4}\frac{G}{H}\frac{m_{\mathrm{orb}}^{\parallel} - m_{\mathrm{orb}}^{\perp}}{\mu_{\mathrm{B}}}, \tag{8}$$

where ξ is the spin-orbit coupling constant, and G and H are the integrals of the density of states. The value of ξ for Fe is ~50 meV,[39] while a rough estimation of G/H is 0.2 for $3d$ transition metals.[40] The difference in the orbital magnetic moments $(m_{\mathrm{orb}}^{\parallel} - m_{\mathrm{orb}}^{\perp})/\mu_{\mathrm{B}}$ is ~0.07 from the present XMCD analysis, and we consequently obtain $K_u \approx 0.18$ meV/atom. On the other hand, the K_u estimated from the simulation results of the magnetization curve in Table II is ~0.10 meV/atom. Although the agreement is not excellent, the order of magnitude is reproduced well, exemplifying semiquantitative accuracy in the present MH curve and XMCD analyses. Note also that the observed K_u value of the thin Fe_4N film is by far larger than the thick γ'-Fe_4N film on $SrTiO_3$ (1.4 μeV/atom) (Ref. 41), that on MgO(001) (2.5 μeV/atom) (Ref. 42), and that on Cu(001) (3.8 μeV/atom) (Ref. 27).

IV. CONCLUSION

In this work, the structural and magnetic properties of iron nitride thin films on Cu(001) were investigated by LEED, STM, XAS, and XMCD. The measurements revealed that the surface of the 1 ML film has a $p4gm(2\times2)$ structure and that the Fe/N composition ratio is 2:1, while the films of more than 1 ML have a composition ratio of 4:1. The magnetic properties of the films are found to be strongly related to their morphology. Especially, the 1 ML film shows strong in-plane magnetic anisotropy, where the perpendicular orbital magnetic moment is almost zero, because the surface N atoms are located almost in the same plane of the topmost Fe layer with strong in-plane chemical bonding. The magnetic moment increases with the film thickness, and that of 3 ML is close to that of bulk γ'-Fe_4N, whereby the structure is quite similar to that of the iron nitride film except for the topmost layer.

*yokoyama@ims.ac.jp

[1] M. Tischer, O. Hjortstam, D. Arvanitis, J. H. Dunn, F. May, K. Baberschke, J. Trygg, J. M. Wills, B. Johansson, and O. Eriksson, Phys. Rev. Lett. **75**, 1602 (1995).

[2] J. H. Dunn, D. Arvanitis, and N. Mårtensson, Phys. Rev. B **54**, R11157 (1996).

[3] N. Nakajima, T. Koide, T. Shidara, H. Miyauchi, H. Fukutani, A. Fujimori, K. Iio, T. Katayama, M. Nývlt, and Y. Suzuki, Phys. Rev. Lett. **81**, 5229 (1998).

[4] P. Srivastava, F. Wilhelm, A. Ney, M. Farle, H. Wende, N. Haack, G. Ceballos, and K. Baberschke, Phys. Rev. B **58**, 5701 (1998).

[5] H. Jenniches, J. Shen, Ch. V. Mohan, S. S. Manoharan, J. Barthel, P. Ohresser, M. Klaua, and J. Kirschner, Phys. Rev. B **59**, 1196 (1999).

[6] D. Schmitz, C. Charton, A. Scholl, C. Carbone, and W. Eberhardt, Phys. Rev. B **59**, 4327 (1999).

[7] A. Ney, P. Poulopoulos, M. Farle, and K. Baberschke, Phys. Rev. B **62**, 11336 (2000).

[8] X. D. Ma, T. Nakagawa, and T. Yokoyama, Surf. Sci. **600**, 4605 (2006).

[9] X. D. Ma, T. Nakagawa, Y. Takagi, M. Przybylski, F. M. Leibsle, and T. Yokoyama, Phys. Rev. B **78**, 104420 (2008).

[10] C. A. F. Vaz, J. A. C. Bland, and G. Lauhoff, Rep. Prog. Phys. **71**, 056501 (2008).

[11] J. Thomassen, F. May, B. Feldmann, M. Wuttig, and H. Ibach, Phys. Rev. Lett. **69**, 3831 (1992).

[12] J. Shen, Z. Gai, and J. Kirschner, Surf. Sci. Rep. **52**, 163 (2004).

[13] Š. Pick, P. Légaré, and C. Demangeat, J. Phys.: Condens. Matter **20**, 075212 (2008).

[14] J. M. D. Coey and P. A. I. Smith, J. Magn. Magn. Mater. **200**, 405 (1999).

[15] E. H. Du Marchie van Voorthuysen, D. O. Boerma, and N. C. Chechenin, Metall. Mater. Trans. A **33**, 2593 (2002).

[16] T. Hinomura and S. Nasu, Hyperfine Interact. **111**, 221 (1998).

[17] T. K. Kim and M. Takahashi, Appl. Phys. Lett. **20**, 492 (1972).

[18] M. Takahashi, H. Shoji, H. Takahashi, H. Nashi, T. Wakiyama, M. Doi, and M. Matsui, J. Appl. Phys. **76**, 6642 (1994).

[19] Y. Sugita, H. Takahashi, M. Komuro, M. Igarashi, R. Imura, and T. Kambe, J. Appl. Phys. **79**, 5576 (1996).

[20] B. C. Frazer, Phys. Rev. **112**, 751 (1958).

[21] J. M. Gallego, S. Y. Grachev, M. C. G. Passeggi, Jr., F. Sacharowitz, D. Ecija, R. Miranda, and D. O. Boerma, Phys. Rev. B **69**, 121404(R) (2004).

[22] J. M. Gallego, S. Y. Grachev, D. M. Borsa, D. O. Boerma, D. Écija, and R. Miranda, Phys. Rev. B **70**, 115417 (2004).

[23] S. Y. Grachev, J. M. Gallego, D. Écija, D. O. Boerma, R. Gonzalez-Arrabal, and R. Miranda, Nucl. Instrum. Methods Phys. Res. B **219-220**, 593 (2004).

[24] J. M. Gallego, D. O. Boerma, R. Miranda, and F. Ynduráin, Phys. Rev. Lett. **95**, 136102 (2005).

[25] C. Navio, J. Alvarez, M. J. Capitan, D. Ecija, J. M. Gallego, F. Yndurain, and R. Miranda, Phys. Rev. B **75**, 125422 (2007).

[26] D. Ecija, E. Jimenez, J. Camarero, J. M. Gallego, J. Vogel, N. Mikuszeit, N. Sacristán, and R. Miranda, J. Magn. Magn. Mater. **316**, 321 (2007).

[27] D. Ecija, E. Jiménez, N. Mikuszeit, N. Sacristán, J. Camarero, J. M. Gallego, J. Vogel, and R. Miranda, Phys. Rev. B **77**, 024426 (2008).

[28] B. T. Thole, P. Carra, F. Sette, and G. van der Laan, Phys. Rev. Lett. **68**, 1943 (1992).

[29] P. Carra, B. T. Thole, M. Altarelli, and X. Wang, Phys. Rev. Lett. **70**, 694 (1993).

[30] M. A. Van Hove, W. Moritz, H. Over, P. J. Rous, A. Wander, A. Barbieri, N. Materer, U. Starke, and G. A. Somorjai, Surf. Sci. Rep. **19**, 191 (1993).

[31] J. B. Pendry, J. Phys. C **13**, 937 (1980).

[32] T. Gejo, Y. Takata, T. Hatsui, M. Nagasono, H. Oji, N. Kosugi, and E. Shigemasa, Chem. Phys. **289**, 15 (2003).

[33] T. Nakagawa, Y. Takagi, Y. Matsumoto, and T. Yokoyama, Jpn. J. Appl. Phys. **47**, 2132 (2008).

[34] J. M. Burkstrand, G. G. Kleiman, G. G. Tibbetts, and J. C. Tracy,

J. Vac. Sci. Technol. **13**, 291 (1976).
[35] S. Ohno, K. Yagyuu, K. Nakatsuji, and F. Komori, Jpn. J. Appl. Phys. **41**, L1243 (2002).
[36] D. Rechenbach and H. Jacobs, J. Alloys Compd. **235**, 15 (1996).
[37] J. Stöhr and H. König, Phys. Rev. Lett. **75**, 3748 (1995).
[38] P. Bruno, Phys. Rev. B **39**, 865 (1989).
[39] J. J. Krebs and W. G. Maisch, Phys. Rev. B **4**, 757 (1971).
[40] D. Weller, J. Stöhr, R. Nakajima, A. Carl, M. G. Samant, C. Chappert, R. Mégy, P. Beauvillain, P. Veillet, and G. A. Held, Phys. Rev. Lett. **75**, 3752 (1995).
[41] K. R. Nikolaev, I. N. Krivorotov, E. D. Dahlberg, V. A. Vas'ko, S. Urazhdin, R. Loloee, and W. P. Pratt, Appl. Phys. Lett. **82**, 4534 (2003).
[42] J. L. Costa-Krämer, D. M. Borsa, J. M. García-Martín, M. S. Martín-González, D. O. Boerma, and F. Briones, Phys. Rev. B **69**, 144402 (2004).